Renewable Energy 103 (2017) 594–605

Contents lists available at ScienceDirect

Renewable Energy

journal homepage: www.elsevier.com/locate/renene

Classification of operating conditions of wind turbines for a class-wise condition monitoring strategy

Jong M. Ha [a], Hyunseok Oh [b, **], Jungho Park [a], Byeng D. Youn [a, *]

[a] Department of Mechanical and Aerospace Engineering, Seoul National University, Seoul, 08826, South Korea
[b] School of Mechanical Engineering, Gwangju Institute of Science and Technology, Gwangju, 61005, South Korea

ARTICLE INFO

Article history:
Received 13 January 2016
Received in revised form
10 October 2016
Accepted 30 October 2016
Available online 2 November 2016

Keywords:
Wind turbine
Condition monitoring system
Fast Fourier transform
Stationary operating conditions
Empirical PDF
Gaussian mixture model

ABSTRACT

Relevant classification of the stationary operating conditions of wind turbines (WTs) aids in the selection of an optimal condition monitoring technique. This paper presents a general method that can be used to classify the operating conditions of WTs in terms of rotor speed and power. In this study, the ideal probability density functions (PDFs) of rotor speed and power are calculated using an analytic WT model and a wind speed profile. To estimate the PDFs of rotor speed and power with field data, two methods are employed: (1) empirical PDF-based and (2) Gaussian mixture model (GMM)-based. The individual PDFs estimated by the two methods are used to quantitatively define the range of the stationary WT operating conditions. The proposed methods and the range of stationary operating conditions established by the methods were evaluated using data from an analytical WT model and an actual 2.5 megawatt WT in the field. In addition, the paper presents the evaluation of the performance of the proposed class-wise condition monitoring strategy when used with vibration signals acquired from a two kilowatt WT testbed. In summary, the proposed strategy and methods are promising for effective condition monitoring of WTs.

1. Introduction

Wind turbines (WTs) often suffer from high maintenance costs and downtime due to undesired failures. Condition-based maintenance can effectively prevent many of these undesired failures and thereby reduce the maintenance costs of WTs [1–3]. However, it is often challenging to evaluate the conditions of WTs using readily-available signal processing techniques (e.g., fast Fourier transform) since condition monitoring signals (e.g., vibration) are inhomogeneous and non-stationary [4]. Due to the uncertain nature of wind profiles, highly variable operating conditions are prevalent during the operation of WTs. Several attempts have been made to use the currently available signal processing techniques for robust condition monitoring of WTs by adaptively using homogeneous condition monitoring signals across a limited range of WT operating conditions. For example, the International Electrotechnical Commission (IEC), an organization that proposes international standards for WT condition monitoring, has recommended that “active power bins” should be used to classify the range of power so that the vibration signals in a particular bin are more homogeneous and exhibit only small variations [5]. Thus, it would be expected that a condition monitoring technique could be effectively used with each bin due to the homogeneous nature of the vibration signals in that “bin.” However, it is well known that vibration characteristics are also dependent on rotational speed [6,7]. Therefore, the IEC's recommendation of using “active power bins” is not appropriate when rotational speed fluctuates. Another organization, DNV GL, proposed a renewables certification that divides the operating conditions of WTs into two parts based on the amount of variation of the WT's speed [8]. In this strategy, computationally efficient signal processing techniques (such as fast Fourier transform) are used only when WTs operate with minimal speed variation. When the WTs operate with frequent speed variation, it is recommended that more advanced condition monitoring techniques be employed [8].

To effectively monitor WTs, some commercial condition monitoring systems also try to use the existing signal processing techniques only when the WTs are operating in a pre-defined narrow range of operating conditions [9]. For example, “Windcon,” developed by SKF, uses the concept of an “active range.” This strategy performs active condition monitoring only while rotor speed and

* Corresponding author.
** Co-corresponding author.
E-mail addresses: hsoh@gist.ac.kr (H. Oh), bdyoun@snu.ac.kr (B.D. Youn).

http://dx.doi.org/10.1016/j.renene.2016.10.071
0960-1481/

power remain in the "active range" [10]. The "Oneprod Wind System," developed by Oneprod, uses wind speed as an additional variable for defining the "active" range for WT monitoring [11]. Although a variety of condition monitoring strategies like these have been proposed that attempt to fully utilize currently available signal processing techniques, it should be noted that to do this, the criteria for the operating conditions of interest for a WT (e.g., the criteria for the "active range" of the "WindCon" method) must be pre-defined by the users. Thus, implementation of the guidelines and options specified by IEC [5], DNV GL [8], SKF [10] and Oneprod [11] is not feasible unless the quantitative criteria for the operating conditions of WTs are given. To the best of our knowledge, there is no practical guideline that quantitatively classifies WT operating conditions to provide an effective range for an optimal WT condition monitoring strategy.

In response to this need, this paper proposes a general method for classification of the operating conditions of WTs in terms of rotor speed and power. The ultimate goal is to use these classifications to establish an optimal strategy for condition monitoring of WTs. Section 2 introduces an analytical WT model that calculates the relationship between input wind speed and power or rotor speed based on a generic control logic for variable-speed WTs. In Section 3, the probability density functions (PDFs) of power and rotor speed are mathematically derived from the analytical WT model to provide a theoretical rationale for the classification method and the criteria for the operating conditions. In Section 4, five distinct classes are developed in such a way that WTs in a particular class have unique operating characteristics, thus leading to homogeneous condition monitoring signals in each class. In particular, to produce the most valuable vibration signal for condition monitoring of WTs, quantitative criteria for the stationary operating condition of WTs are defined, while considering inherent randomness in the performance of WTs. Section 5 presents two case studies: (1) a WT model with various levels of average wind speed and (2) an actual 2.5 megawatt WT in the field. Section 6 discusses the applicability of the proposed classification-based condition monitoring strategy to the industry and presents condition monitoring results for a two kilowatt WT testbed under various operating conditions. This paper concludes with a summary and suggestions for future work, outlined in Section 7.

2. Analytical modeling of WT performance

Different control logic strategies are implemented to achieve optimal performance in variable-speed WTs [12]. As illustrated in Fig. 1, in Region 1, the wind speed is less than the "cut-in" wind speed ($v_{cut\text{-}in}$). In this region, the wind energy is considered to be insufficient to produce power. Consequently, the WT is directed not to generate power, and instead stays in an idle mode. When the wind speed exceeds the cut-in wind speed, the rotor starts to rotate at the cut-in rotor speed ($w_{cut\text{-}in}$). In Region 2, the output power of the WT can be characterized as being proportional to the cube of the wind speed [13]. The rotor speed is controlled to maximize the efficiency of the WT's energy production in such a way that the rotor speed can be approximated as being linearly proportional to the wind speed [14]. When the wind speed becomes high enough to generate the rated power (P_{rated}) and the rated rotor speed (w_{rated}) of the WT, the blade pitch is controlled to maintain the power and rotor speed at constant levels (Region 3). Based on the WT control logic outlined here, the relationship between the wind speed (v) and normalized power (P), or normalized rotor speed (w), can be represented as:

$$P = \begin{cases} 0 & v < v_{cut-in} \\ (v/v_{rated})^3 & v_{cut-in} \le v < v_{rated} \\ 1 & v_{rated} \le v \end{cases} \quad (1)$$

$$w = \begin{cases} 0 & v < v_{cut-in} \\ v/v_{rated} & v_{cut-in} \le v < v_{rated} \\ 1 & v_{rated} \le v \end{cases} \quad (2)$$

On the other hand, it has been reported that any engineered system including WTs has considerable uncertainties due to several issues, such as randomness in geometry, material property and loading (e.g., stochastic nature of the wind property) [15,16]. Based on the work of Tondan and Zhigang, power and rotor speed with random noise can be defined by incorporating Gaussian noise as [17]:

$$P_n = P + \varepsilon_P \quad (3)$$

$$w_n = w + \varepsilon_w \quad (4)$$

where ε_p and ε_w represent the Gaussian noise with a mean of zero and a standard deviation of σ (i.e., $\varepsilon_p \sim N(0, \sigma_P^2)$, and $\varepsilon_w \sim N(0, \sigma_w^2)$).

To calculate the power and rotor speed using the WT model, wind speed (v) must be known. Prior research recommends that wind distribution should be assumed to follow a Rayleigh distribution whose CDF (F_v) and PDF (f_v) can be defined as [18,19]:

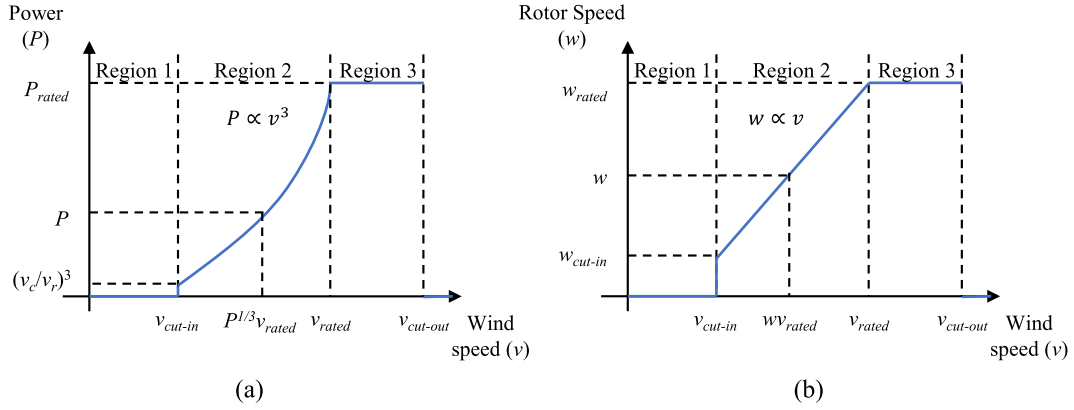

Fig. 1. Region of wind speed for control of WTs. (a) wind speed-power relationship. (b) wind speed-rotor speed relationship.

$$F_v(v;\bar{v}) = 1 - e^{-\frac{\pi}{4}\left(\frac{v}{\bar{v}}\right)^2}, v \geq 0 \tag{5}$$

$$f_v(v;\bar{v}) = \frac{\pi}{2}\frac{v}{(\bar{v})^2}e^{-\frac{\pi}{4}\left(\frac{v}{\bar{v}}\right)^2}, v \geq 0 \tag{6}$$

where $\bar{v}$ stands for average wind speed. The IEC 61400-1 certification provides three representative average wind speeds (i.e., $\bar{v}$=7.5, 8.5, and 10 m/s) that should be considered for Eqs. (5) and (6) to explain the general behavior of wind at different sites [20]. Rayleigh distributions with average wind speeds of 7.5 m/s, 8.5 m/s, and 10 m/s are compared in Fig. 2.

3. Mathematical derivation of the PDF of power and rotor speed

This section proposes a two-step procedure to derive the statistical description (i.e., PDF) of WT performance in terms of power and rotor speed. This procedure consists of (1) a uncertainty propagation technique to consider propagation of uncertainty in wind speed and (2) convolution of two main sources of the randomness, such as uncertain system performance and Gaussian noise. Detailed procedures for determining the PDFs of the power and the rotor speed are provided in Sections 3.1 and 3.2, respectively.

3.1. The PDF of power

In this work, a random variable transformation technique was employed to show the PDF of power in terms of the PDF of wind speed. Mathematically, when y (e.g., power) is a function of a random variable x (e.g., wind speed) with a relationship of $y = g(x)$, the uncertainty of x is propagated to the one of y, formulating a cumulative distribution function (CDF), (F_Y) as [21]:

$$F_Y(y) = P(Y \leq y) = P(g(x) \leq y) = P(X \in B_y), \tag{7}$$

where

$$B_y = \{x \in \mathrm{IR} : g(x) \leq y\} \tag{8}$$

Using the random variable transformation technique, the CDF of the power from Eq. (1) becomes:

$$F_P(P) = \begin{cases} 0 & P < 0 \\ \mathrm{P}(v \leq v_{cut-in}) = 1 - e^{-\frac{\pi}{4}\left(\frac{v_{cut-in}}{\bar{v}}\right)^2} & 0 \leq P < (v_{cut-in}/v_{rated})^3 \\ \mathrm{P}\left(v \leq P^{1/3}v_{rated}\right) = 1 - e^{-\frac{\pi}{4}\left(\frac{P^{1/3}v_{rated}}{\bar{v}}\right)^2} & (v_{cut-in}/v_{rated})^3 \leq P < 1 \\ 1 & 1 \leq P \end{cases} \tag{9}$$

In (9), jump discontinuities exist for C_0 (when $P = 0$) and C_1 (when $P = 1$):

$$C_0 = F_P(0) - \lim_{P \to 0^-} F_P(P) = 1 - e^{-\frac{\pi}{4}\left(\frac{v_{cut-in}}{\bar{v}}\right)^2} \tag{10}$$

$$C_1 = F_P(1) - \lim_{P \to 1^-} F_P(P) = 1 - \left(1 - e^{-\frac{\pi}{4}\left(\frac{v_{rated}}{\bar{v}}\right)^2}\right) = e^{-\frac{\pi}{4}\left(\frac{v_{rated}}{\bar{v}}\right)^2} \tag{11}$$

The differentiation of (9) with respect to P becomes:

$$\tilde{f}_P(P) = \begin{cases} \frac{\pi}{6}\left(\frac{v_{rated}}{\bar{v}}\right)^2 P^{-1/3} e^{-\frac{\pi}{4}\left(\frac{P^{1/3}v_{rated}}{\bar{v}}\right)^2} & (v_{cut-in}/v_{rated})^3 < P < 1 \\ 0 & \text{otherwise} \end{cases} \tag{12}$$

The PDF of the power (f_P) is obtained by combining Eq. (12) with Eqs. (10) and (11):

$$f_P(P) = C_0\delta(P) + C_1\delta(P-1) + \tilde{f}_P(P) \tag{13}$$

Next, the Gaussian noise term (ε_P) is added to Eq. (13) to incorporate the effect of the inherent randomness in WTs. The PDF of a sum of two random variables is calculated by convolution [21]. The PDF of the power with the noise term is presented as:

$$\begin{aligned} f_{Pn}(P) &= (f_P * \varepsilon_P)(P) = \int_{-\infty}^{\infty} f_P(y) \times \varepsilon_P(P-y)dy \\ &= \int_{-\infty}^{\infty} f_P(y) \times \frac{1}{\sigma_P\sqrt{2\pi}} e^{-\frac{(P-y)^2}{2\sigma_P^2}} dy \\ &= \frac{C_0}{\sigma_P\sqrt{2\pi}} e^{-\frac{P^2}{2\sigma_P^2}} + \frac{C_1}{\sigma_P\sqrt{2\pi}} e^{-\frac{(P-1)^2}{2\sigma_P^2}} + \tilde{f}_{Pn}(P), \end{aligned} \tag{14}$$

where $\tilde{f}_{Pn}(P)$ is calculated through the following equation:

$$\begin{aligned} \tilde{f}_{Pn}(P) &= \int_{-\infty}^{\infty} \tilde{f}_P(y) \times \frac{1}{\sigma_P\sqrt{2\pi}} e^{-\frac{(P-y)^2}{2\sigma_P^2}} dy \\ &= \int_{(v_{cut-in}/v_{rated})^3}^{1} \frac{\pi}{6}\left(\frac{v_{rated}}{\bar{v}}\right)^2 y^{-1/3} e^{-\frac{\pi}{4}\left(\frac{y^{1/3}v_{rated}}{\bar{v}}\right)^2} \\ &\quad \times \frac{1}{\sigma_P\sqrt{2\pi}} e^{-\frac{(P-y)^2}{2\sigma_P^2}} dy \end{aligned} \tag{15}$$

In Eq. (14), the PDF was defined as the sum of three terms. The first two terms were derived from the impulse function with the magnitudes of C_0 and C_1 near zero and the rated power, respectively. The power in the mid-range is dominated by the third term in Eq. (14), which cannot be calculated analytically. Several

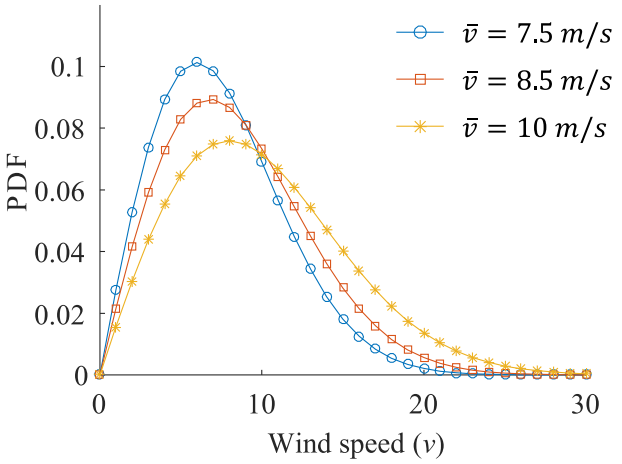

Fig. 2. The probability density functions (PDFs) of wind speeds modeled by Rayleigh distribution with the average wind speeds of 7.5 m/s, 8.5 m/s, and 10 m/s.

numerical integration methods can be used, such as the Trapezoidal rule and adaptive Gauss-Kronrod quadrature [20, 22]. Fig. 3 (a) and (b) respectively show the CDF and PDF of the power where the noise term is not considered. It is noteworthy that C_0 and C_1, which are generated from the idle and pitch control mode of the WT, are represented as discontinuities of the CDF (C_0 and C_1) in Fig. 3 (a) and as impulse functions with magnitude of C_0 and C_1 in Fig. 3 (b). The PDF of the power subjected to uncertainties is shown in Fig. 3 (c). The standard deviation of the Gaussian noise was set to be 2.5% of the rated operating condition (i.e., $\sigma_p = 0.025$) for the study [23]. The discontinuities were reconstructed as clusters around zero and rated power, as shown in Fig. 3 (c).

3.2. The PDF of rotor speed

Identical procedures were used in our study to define the PDF of rotor speed. Using the random variable transformation technique, the CDF of the rotor speed becomes:

$$F_w(w) = \begin{cases} 0 & w<0 \\ \mathrm{P}(v \le v_{cut-in}) = 1 - e^{-\frac{\pi}{4}\left(\frac{v_{cut-in}}{\bar{v}}\right)^2} & 0 \le w < v_{cut-in}/v_{rated} \\ \mathrm{P}(v \le wv_{rated}) = 1 - e^{-\frac{\pi}{4}\left(\frac{wv_{rated}}{\bar{v}}\right)^2} & v_{cut-in}/v_{rated} \le w < 1 \\ 1 & 1 \le w \end{cases} \tag{16}$$

The PDF of the rotor speed (f_w) is presented as:

$$f_w(w) = C_0\delta(w) + C_1\delta(w-1) + \tilde{f}_w(w) \tag{17}$$

where C_0 at $w = 0$ and C_1 at $w = 1$ are as defined in Eqs. (10) and (11). The third term is obtained by differentiating F_w with respect to w.

$$\tilde{f}_w(w) = \begin{cases} \frac{\pi}{2}\left(\frac{v_{rated}}{\bar{v}}\right)^2 we^{-\frac{\pi}{4}\left(\frac{wv_{rated}}{\bar{v}}\right)^2} & v_{cut-in}/v_{rated} < w < 1 \\ 0 & \text{otherwise} \end{cases} \tag{18}$$

The PDF of the rotor speed with uncertainties then becomes:

$$f_{wn}(w) = (f_w * \varepsilon_w)(w) = \frac{C_0}{\sigma_w\sqrt{2\pi}}e^{-\frac{w^2}{2\sigma_w^2}} + \frac{C_1}{\sigma_w\sqrt{2\pi}}e^{-\frac{(w-1)^2}{2\sigma_w^2}} + \tilde{f}_{wn}(w) \tag{19}$$

where $\tilde{f}_{wn}(w)$ is calculated using the following equation.

$$\tilde{f}_{wn}(w) = \int_{v_{cut-in}/v_{rated}}^{1} \frac{\pi}{2}\left(\frac{v_{rated}}{\bar{v}}\right)^2 ye^{-\frac{\pi}{4}\left(\frac{yv_{rated}}{\bar{v}}\right)^2} \times \frac{1}{\sigma_w\sqrt{2\pi}}e^{-\frac{(w-y)^2}{2\sigma_w^2}}dy \tag{20}$$

The CDF and PDF of the rotor speed, and the PDF of the rotor speed with uncertainties are shown in Fig. 4 (a)-(c).

4. Classification of the operating conditions of a WT

This section proposes a method for classification of WT operating conditions. Then, quantitative criteria for the stationary operating condition are defined by using the properties of distribution of power and rotor speed, which were outlined in Section 3. Empirical PDF and Gaussian mixture model (GMM) techniques are employed to enable practical use of the proposed method in the field where exact PDF equations are not provided.

4.1. A classification method for operating conditions of a WT

As illustrated in Fig. 5, the proposed methods aim to classify the operating conditions of WTs into five classes in terms of the rotor speed and the output power. Boundaries between the stationary and non-stationary operating conditions for power and rotor speed are represented as C_p and C_w, respectively. When both the power and the rotor speed are greater than C_p and C_w simultaneously, the data collected for this operating regime is assigned to Class I. In this

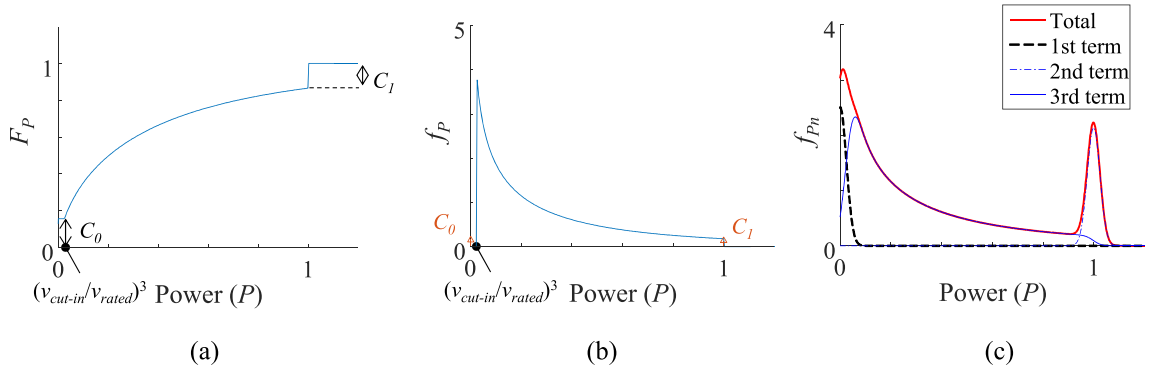

Fig. 3. The CDF and PDF of power. (a) the CDF of power. (b) the PDF of power. (c) the PDF of power with uncertainties.

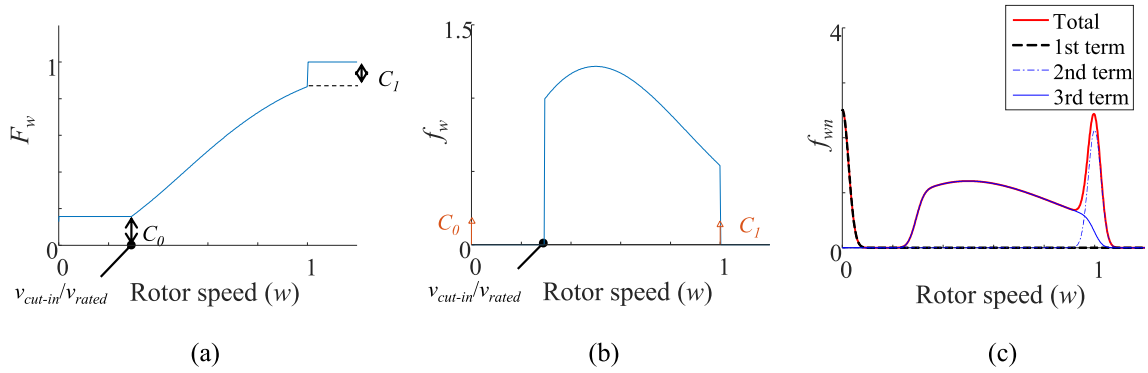

Fig. 4. The CDF and PDF of rotor speed. (a) the CDF of rotor speed. (b) the PDF of rotor speed. (c) the PDF of rotor speed with uncertainties.

class, power and rotor speed should remain nominally constant at their rated values due to the pitch control of the WT. For this class, cost-effective signal processing techniques, such as fast Fourier transform and order analysis can serve as efficient tools for condition monitoring of the WT, since the condition monitoring signal is stationary and homogeneous. In Class II, WTs operate in a quasi-stationary operating condition with varying power production, despite the nominally constant rotor speed. This scenario can occur due to rapidly varying wind properties or through pitch and yaw error in the WT [19]. In this case, the energy contained in the measured condition monitoring signal can be dependent to the varying power profile [24,25]. Next, non-stationary operating conditions of WTs were defined as Class III where both the rotor speed and the power were significantly varying below C_p and C_w. In this case, the condition monitoring signal requires an advanced signal processing technique applicable to the varying operating conditions. The operating conditions of WTs in idle mode were defined as Class V, where the rotor speed and power are zero. Class IV is assigned for transient operating conditions between Class III and Class V, where rotor speed varies below the cut-in rotor speed, and power is zero. In Class IV and Class V, the condition monitoring signal is not likely to include meaningful information with respect to condition monitoring of the WTs. Fig. 6 shows an illustrative example of the operating conditions of a WT for each class, where C_p and C_w were set to be equal for simplified representation.

4.2. Definition of quantitative classification criteria

This section defines quantitative criteria that define boundaries between stationary and non-stationary operating conditions of WTs (i.e., C_p and C_w). These boundaries are required for accurate classification. As shown in Figs. 3 (c) and 4 (c), clusters are formed around the rated operating condition due to the pitch control used by WTs when there is enough wind speed to warrant such control. The boundaries between the stationary and non-stationary operating conditions of WTs (i.e., C_p and C_w) can be defined as values that separate the clusters formed around the rated power and rotor speed. This section proposes two methods to define the appropriate values of C_p and C_w that satisfy the following conditions: (1) C_p and C_w should be small enough to obtain as much data as possible in Class I, and (2) C_p and C_w should not be excessively small such that they guarantee stationary operating conditions in Class I.

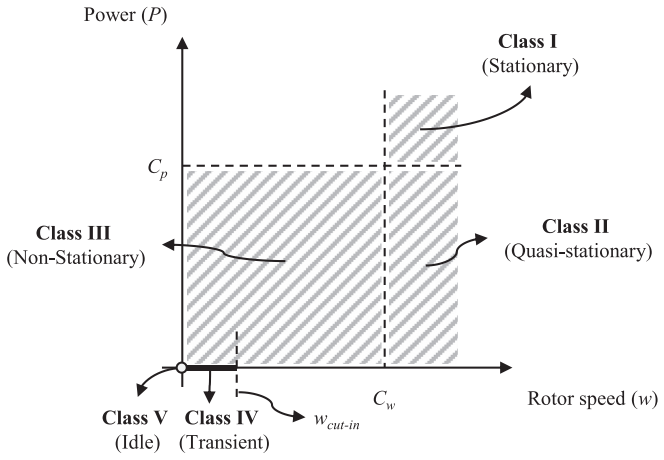

Fig. 5. The proposed classification rule for operating conditions of a WT.

4.2.1. Method 1: identification of minimum probability density using an empirical PDF

Boundaries between stationary and non-stationary operating conditions can be defined based on the properties of the distribution of power and rotor speed. As the power (P) and the rotor speed (w) approach to the rated values, their probability densities (i.e., f_p and f_w) decrease where the noise term is not incorporated as shown in Figs. 3 (b) and 4 (b). When the PDFs of the power and the rotor speed incorporate inherent randomness, clusters are formed around the rated values by convolution of the noise term and the impulse function with the magnitude of C_1, eventually increasing probability densities (See "Total" lines in Figs. 3 (c) and 4 (c)). As a result, the PDFs of power and rotor speed should have a concave form around the rated operating condition. Theoretical boundaries between stationary and non-stationary operating conditions can be defined as the point where the PDFs of power and rotor speed are minimized around the rated operating condition. Although it seems to be straightforward to find the minimum of the PDF around the rated operating condition, it is challenging to do this in field settings where the exact equations for the PDFs of power and rotor speed are not given. To solve this challenge, this study employed an empirical PDF. The empirical PDF is a data-oriented empirical measure of the probability distribution of a random variable, which is widely used in real field because of easy implementation and a general convergence property as a non-parametric density estimator [26]. The empirical PDF can be derived by numerical differentiation of an empirical CDF as:

$$f(x) = \frac{F(x+\Delta x) - F(x)}{\Delta x} \tag{21}$$

where $F(x)$ and x represent the empirical CDF and WT performance, respectively; and Δx is the difference between two adjacent values. The empirical CDF ($F(x)$) can be defined as [27]:

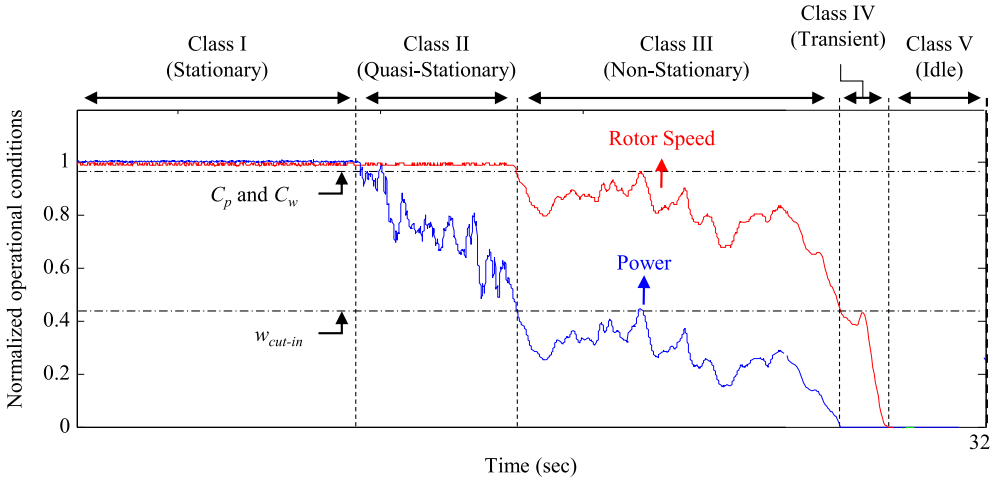

Fig. 6. Sample results of the proposed method for classification of operating conditions of a WT.

$$F(x) = \frac{1}{N_s}\sum_{i=1}^{N_s} 1\{x_i \le x\} \tag{22}$$

where N_s is the number of samples; x_i is the measured WT performance at the ith sample point ($i = 1, \ldots, N_s$); and $1\{A\}$ is the indicator function that computes one only if the logic A is satisfied.

Fig. 7 represents the relative histogram and the empirical PDFs for power and rotor speed around the rated operating condition that were calculated from the analytical WT model with an average wind speed of 7.5 m/s. The sampling rate was assumed to be one sample per second, and one-year of data was used. From the figure, it can be seen that C_p and C_w could be quantitatively defined by employing the empirical PDF.

Empirical PDFs, non-parametric density estimator, have been widely used in actual applications due to easy implementation and low computational cost compared to other density estimators. Theoretically, with the infinite number of data points, an empirical PDF will converge to the PDF of a population while having a general property as a density estimator [26]. In reality, it is infeasible to collect the infinite number of data points. Thus, a general guideline should be given to define the appropriate number of data points for Method 1. The issue was addressed in several studies [33]. As an example, the ASME international standard suggests that the minimum number of data points should be calculated by Ref. [34]:

$$n = \left(\frac{3\sigma_o}{E}\right)^2 \tag{23}$$

where σ_o is the estimate of the standard deviation of the population and E is the maximum acceptable difference between the true mean and the sample mean. When σ_o is assumed to be 0.025 (difference between σ_p and σ_w in Eqs. (14) and (19)) and E is set to be 1% of the operating condition for an accurate estimation, the minimum number of data points required for Method 1 is 56.25. This amount of data corresponds to about 0.4 days of WT operation if a single data point is collected every 10 min [35].

Most of the guidelines for the determination of the appropriate number of data points including Eq. (23) assume that the probability distribution of the population follows a single-modal

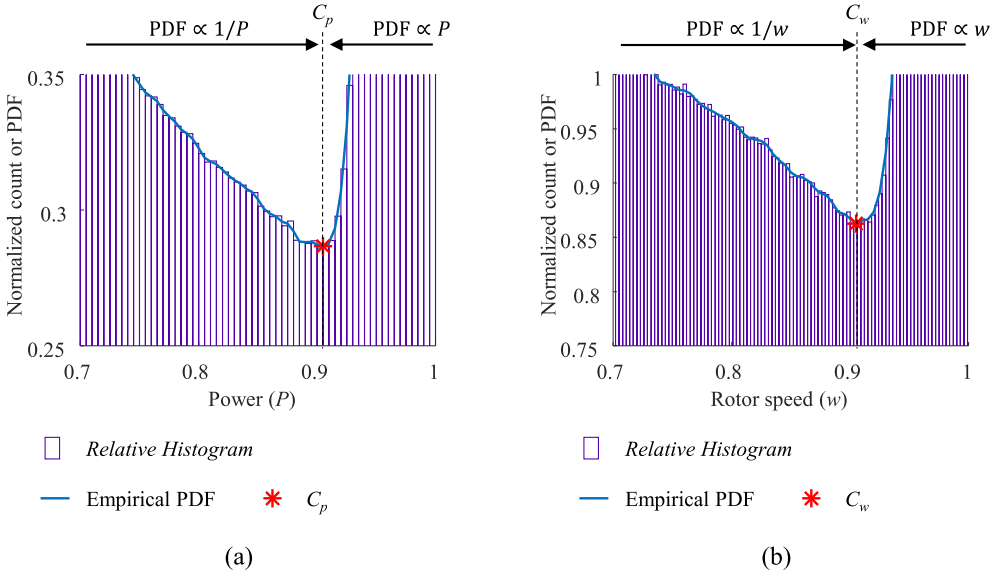

Fig. 7. The PDF for the operating conditions of the WT model around the rated condition where an average wind speed of 7.5 m/s was used. (a) power. (b) rotor speed.

Gaussian distribution. However, the probability distribution of the operating data of WTs generally follows a multi-modal Gaussian distribution. As shown in Section 5, at least, five Gaussian distributions were needed for a proper fitting of the probability distribution of the WT operating data. Consequently, the empirical PDFs require much longer period of time (e.g., 4 days = 0.4 days × 10 safety factor).

4.2.2. Method 2: deconvolution of stationary data using a Gaussian mixture model (GMM)

Criteria for the stationary operating condition of power and rotor speed (C_p and C_w) can be defined based on statistical moments (e.g., mean and standard deviation) of the clusters around the rated operating conditions of the WTs. A statistical moment of the clusters can be approximated by using a Gaussian mixture model (GMM) as it is widely used to fit multi-modal distributions [28]. A GMM can be expressed as a combination of multiple Gaussian distributions:

$$f(x;\theta) = \sum_{k=1}^{K} w_k N(x;\mu_k,\sigma_k) \tag{24}$$

where K is the number of Gaussian distributions used to fit the given distribution; w_k is the weight of the kth Gaussian distribution; and $N(x;\mu_k,\sigma_k)$ is the kth Gaussian distribution with the mean of μ_k and the standard deviation of σ_k,. The PDF of a Gaussian distribution with the mean of μ_k and the standard deviation of σ_k is defined as:

$$N(x;\mu_k,\sigma_k) = \frac{1}{\sigma_k\sqrt{2\pi}} e^{-\frac{(x-\mu_k)^2}{2\sigma_k^2}} \tag{25}$$

This study estimated the optimal Gaussian mixture parameters (i.e., w_k, μ_k, and σ_k, where $i = 1, \ldots, K$) to achieve the maximum likelihood function by employing an expectation and maximization (EM) algorithm, as is commonly used for the GMM [29]. Fig. 8 represents an example of the power and rotor speed of the analytical WT model fitted using the GMM with four Gaussian distributions (i.e., $K = 4$). It can be seen that the clusters located around the rated power and rotor speed were appropriately fitted by the last Gaussian distribution of the GMM. This is marked as '#4' in Fig. 8.

The more distributions employed, the better the fitting capability of the GMM. However, one limitation of the GMM with EM is that the convergence can be extremely slow as the number of distributions (K) increases [29]. Moreover, an extremely large number of distributions can cause a single-modal distribution to be fitted by two or more distributions of the GMM to achieve better fitting results. This is an undesirable case because the purpose of employing the GMM in this study is to fit the clusters formed around the rated power and rotor speed with a single Gaussian distribution to estimate the statistical moments of data in the stationary operating condition. Thus, this paper recommends the use of the minimum number of distributions as long as the clusters formed around the rated operating condition are properly fitted.

To define the criteria for the stationary operating condition (C_p and C_w) based on the statistical moments of the last distribution of the GMM, the three sigma rule was employed. The three sigma rule is that 99.87% of data is within three standard deviations of the mean. Because the desired situation is to secure as much data as possible in Class I, the three sigma rule can be used for defining the conservative criteria for the stationary operating condition. Based on the three sigma rule, C_p and C_w can be defined as:

$$C_p = \mu_{K,p} - 3\sigma_{K,p} \tag{26}$$

$$C_w = \mu_{K,w} - 3\sigma_{K,w} \tag{27}$$

where $\mu_{K,p}$ and $\mu_{K,w}$ are the means of the last Gaussian distribution for power and rotor speed, respectively; and $\sigma_{K,p}$ and $\sigma_{K,w}$ are the standard deviations of the last Gaussian distribution for power and rotor speed, respectively.

5. Case studies

This paper presents two case studies to demonstrate the proposed classification method. First, classification of operating conditions was demonstrated using data calculated from an analytical WT model with various levels of wind speed. Second, field data measured from a 2.5 megawatt WT was used for classification.

5.1. Case study with data calculated from the analytical WT model

This paper considers WT models with different levels of average wind speeds (i.e., $\bar{v}$= 7.5, 8.5, and 10 m/s). Fig. 9 presents results corresponding to the empirical PDF of power and rotor speed. Solid vertical lines and dashed vertical lines represent the results from Methods 1 and 2, respectively. As the average level of wind speed increases, clusters around the rated operating condition of the WT showed a dense distribution with large populations due to the high wind speed. Table 1 summarizes the criteria for the stationary operating condition as defined by Methods 1 and 2. The criteria derived by Method 1 were unstable while having large standard deviations over three wind speeds. On the other hand, the criteria defined by Method 2 were in proportional to the level of wind speed while having small standard deviations.

Because it is beneficial for condition monitoring to obtain as many stationary vibration signals as possible, the criteria for the stationary operating condition can be defined as the minimum value between the results from Methods 1 and 2. However, the stationary operating condition is not likely to be guaranteed if the range of the stationary operating condition is set to be too large. In this case study, Method 1 required more data defined as Classes I and II than Method 2 does. Nevertheless, homogeneity of the vibration signals in Classes I and II defined using Method I should be carefully checked for ensuring the effective condition monitoring. A homogeneity evaluation method will be described in Section 6.1.

5.2. Case study with data measured from a 2.5 megawatt WT

This paper used data from a 2.5 megawatt WT in the Yeongheung wind farm, which is in the west side of the Republic of Korea. For the second case study, operating data from the WT (e.g., wind speed, rotor speed, and output power) were collected for one year at a one-Hz sampling rate. Collected data are represented in Fig. 10 (a) and (b) as three dimensional histograms describing rotor speed and power. The principal operating mode of the WT was the idle control mode, which can be seen in the notable peak in Fig. 10 (a) where both the power and rotor speed are around zero. When the data in the idle control mode was excluded, an additional cluster appeared around the rated power and rotor speed, as shown in Fig. 10 (b). This cluster can be regarded as the data in the stationary operating condition, which was defined as Class I.

Fig. 11 (a) and (b) represent histograms for power and rotor speed data measured from the WT, respectively; Table 2 summarizes criteria for the stationary operating condition (i.e., C_p and C_w) as defined using Methods 1 and 2, respectively. Using the second

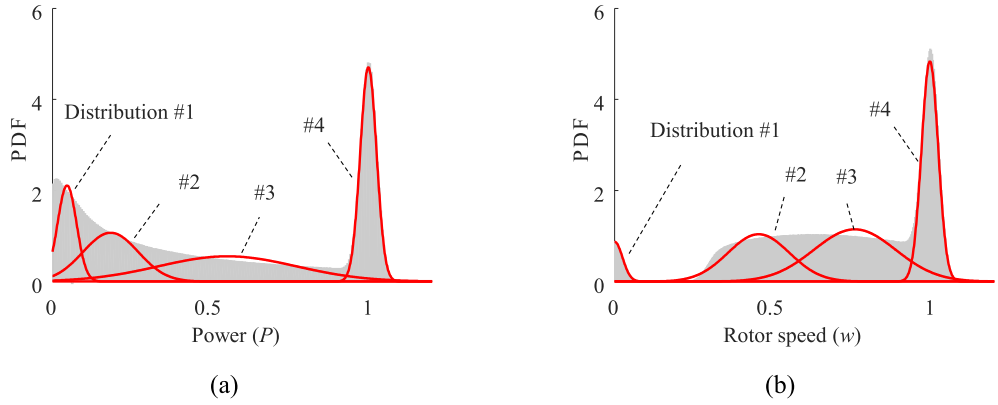

Fig. 8. The PDF for operating conditions using a WT model fitted by a Gaussian mixture model with four Gaussian distributions where average wind speed of 7.5 m/s was used. (a) power. (b) rotor speed.

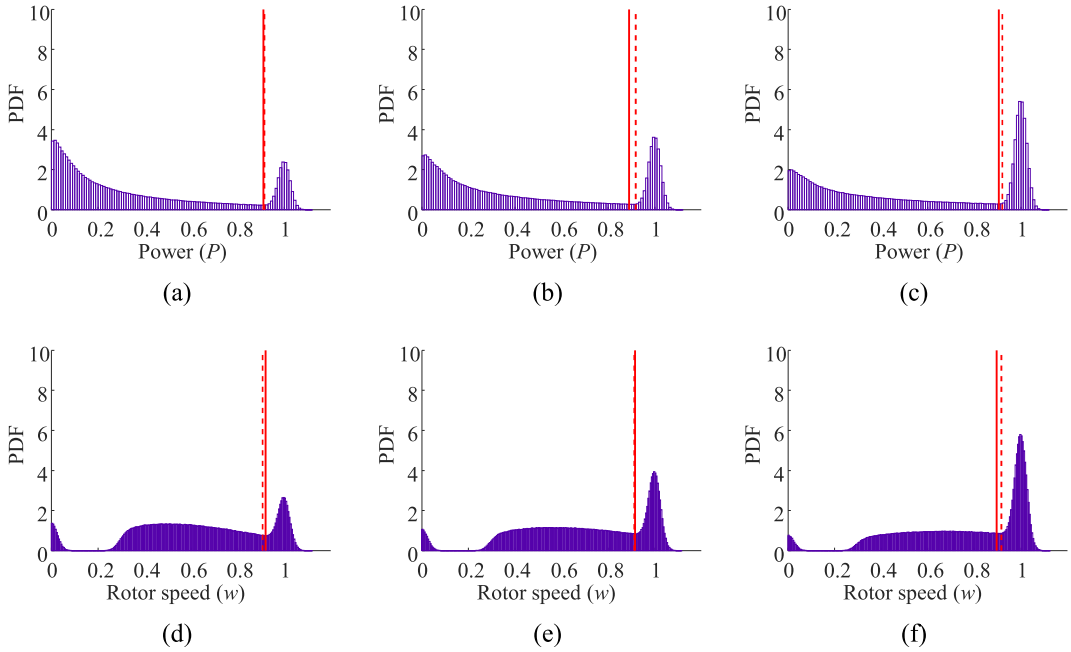

Fig. 9. Criteria for the stationary operating condition where solid vertical lines represent the results from Method 1 and dashed vertical lines represent the results from Method 2. (a)–(c) power with average wind speed of 7.5, 8.5, and 10 m/s, respectively. (d)–(f) rotor speed with average wind speed of 7.5, 8.5, and 10 m/s, respectively.

method, it was found that at least five and four Gaussian distributions should be employed for the GMM to successfully fit the clusters formed around the rated power and rated rotor speed, respectively. In this case, results from the first method were smaller than those from the second method. Method 1 was thus used to define the criteria for the stationary operating condition to obtain the greatest amount of possible homogeneous signals for condition monitoring. Note that if the homogeneity of the condition

Table 1
Classification criteria defined using Methods 1 and 2 for the WT model with different levels of uncertainties.

Criteria		Method 1 (Empirical PDF)	Method 2 (GMM)
C_p	$v = 7.5$ m/s	0.910	0.915
	$v = 8.5$ m/s	0.890	0.918
	$v = 10$ m/s	0.905	0.920
	Mean	0.902	0.918
	Standard deviation	0.010	0.003
C_w	$v = 7.5$ m/s	0.920	0.907
	$v = 8.5$ m/s	0.915	0.912
	$v = 10$ m/s	0.895	0.916
	Mean	0.910	0.912
	Standard deviation	0.013	0.005

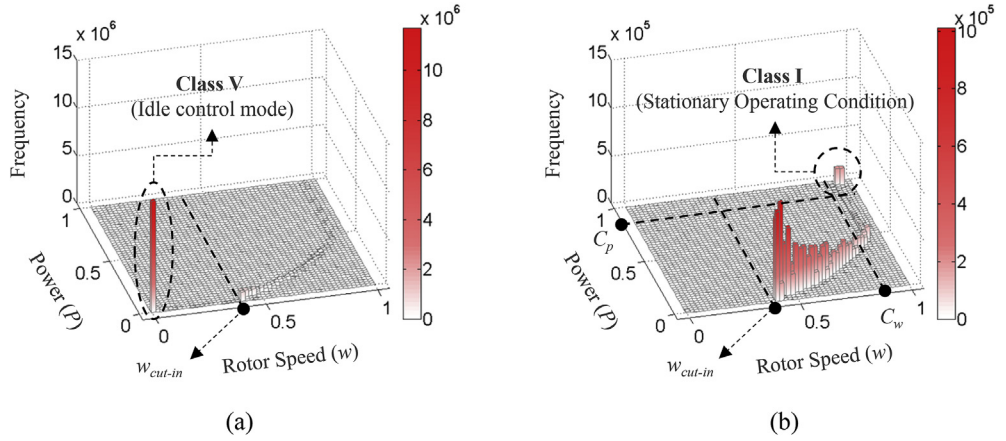

Fig. 10. A three-dimensional histogram of power and rotor speed of the on-shore WT for one year. (a) full data. (b): data in which power is zero are filtered out.

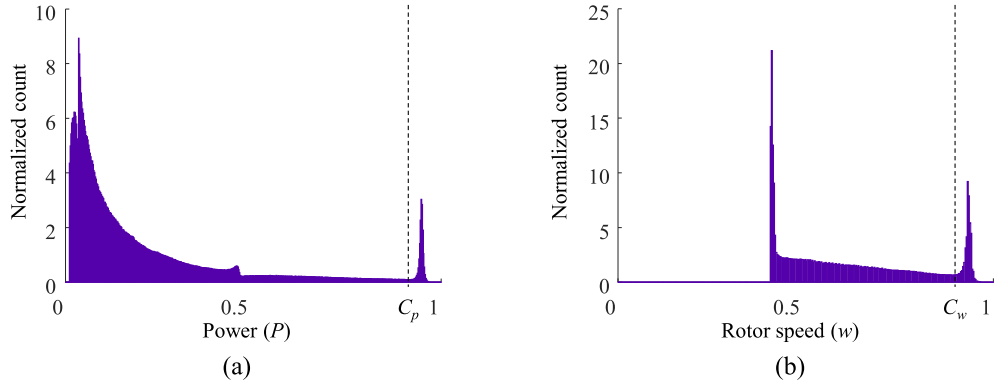

Fig. 11. A relative histogram of the operating conditions of a WT for one year. Data in which power is equal to zero are filtered out for graphically tidy representation. (a) power. (b) rotor speed.

monitoring signals is not guaranteed, the classification criteria should be altered to use the results from Method 2.

The ratios of data observed for each of the defined classes are shown in Fig. 12. It turned out that 2.85% of data were classified into Class I, which is thought to be most effective for condition monitoring. This amount of data corresponds to 41 min per day, on average. Class II, the quasi-stationary operating condition, consists of 5.65% of data, which corresponds to 81 min per day, on average. The WT operates in a nominally stationary rotational speed in both Class I and Class II. Thus, condition monitoring can be performed with a readily available, cost-effective signal processing techniques for data from about 122 min on average per day, without much concern about speed variation. However, power variation should also be considered for Class II data if the energy variation of the condition monitoring signal is evaluated and found to be large. It is also worth noting that Class IV and Class V, which may be trivial for condition monitoring of WTs, comprised an extremely large proportion of data (i.e., about 31% and 26% for Classes IV and V, respectively). This implies that unnecessary computational cost can be saved by excluding Class IV and Class V from the datasets to be processed for condition monitoring. Likewise, Class III, which has large variations in rotational speed and power, accounted for 34% of data.

Table 2
The criteria for defining the stationary operating condition of the on-shore WT, as defined based on the two proposed methods.

Criteria	Method 1 (Empirical PDF)	Method 2 (GMM)
C_p	0.915	0.920
C_w	0.890	0.920

6. Validation study for classification of stationary operating conditions

To discuss the applicability of the proposed classification-based condition monitoring strategy, it is worth performing fault diagnostics under the various operating conditions that were defined

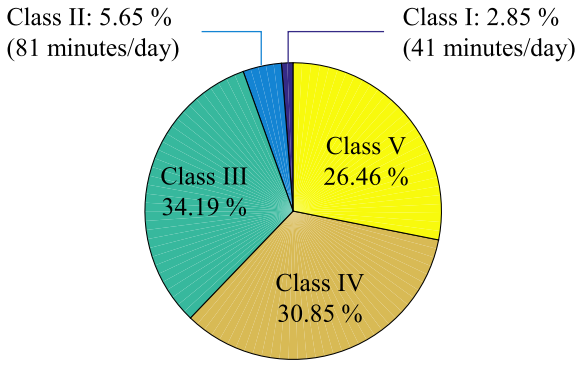

Fig. 12. Classification results of the WT data.

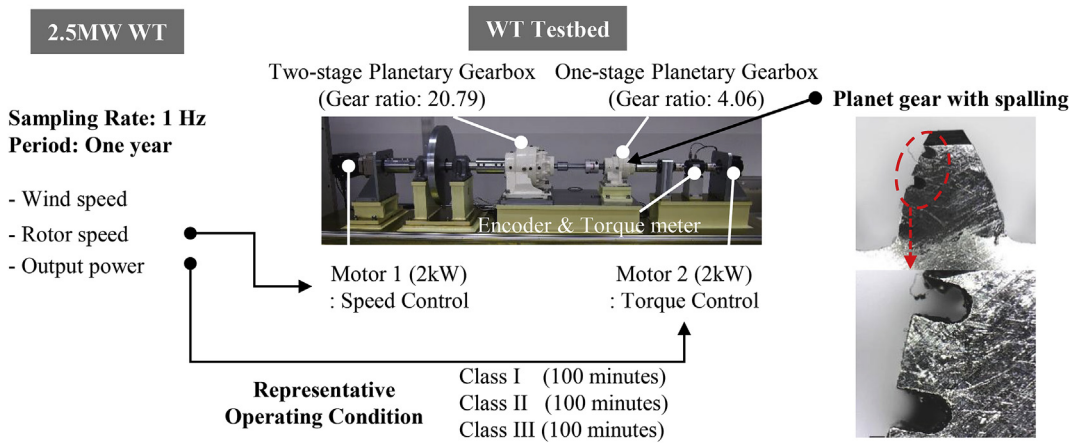

Fig. 13. Overview of testbed operation.

in this paper (i.e., Class I and II). However, it was not easy to gather condition monitoring signals from anomaly conditions from actual WTs. As an alternative, the research described in this paper employed a two kilowatt WT testbed. This testbed helps analyze the effect of the operating conditions on condition monitoring performance. An overview of the testbed is shown in Fig. 13. Among the two gearboxes available, condition monitoring was performed for the one-stage planetary gearbox, which has gear ratio of 4.06. The one-stage planetary gearbox contains three planet gears with 31 teeth on each. The sun gear and the ring gear of the gearbox have 31 teeth and 95 teeth, respectively. For testbed operation, three representative operating conditions, representing Class I, Class II and Class III were measured for the 2.5 megawatt WT, as shown in Fig. 14. Next, rotor speed and scaled torque were used for a control profile of the WT testbed. The vibration signal was measured using an accelerometer attached to the top of the gearbox with a sampling ratio of 25.6 kHz. The vibration signal from 100 min of operation was divided into 100 datasets for vibration-based fault diagnostics with 1-min vibration signals in each dataset. After the tests, the homogeneity of the vibration signals in each class was evaluated using a similarity test with a cross-correlation function. Finally, vibration-based condition monitoring was performed for each class.

6.1. Homogeneity evaluation of the vibration signals

Provided that the vibration signal in a class is homogeneous, the vibration signal should have a similar vibration pattern and energy as long as the meshing condition of the gearbox remains identical. In this research, the homogeneity of the vibration signals in each class was evaluated by investigating the level of similarity of the vibration signals across datasets by means of a cross-correlation metric. Homogeneity of vibration signals was obtained by an average of similarities evaluated from the number of the possible combinations of 100 datasets in each class, ${}_{100}C_2$ (=4950). Fig. 15 compares the level of homogeneity of vibration signals for each class. For readability, vibration signals corresponding to only 10 datasets are aligned in Fig. 15. As can be seen from the figure, the level of homogeneity of vibration signals in Classes I and II was greater than the level observed for vibration signals under Class III. Interestingly, the level of homogeneity of vibration signals in Classes I and II was similar despite the power variation in Class II.

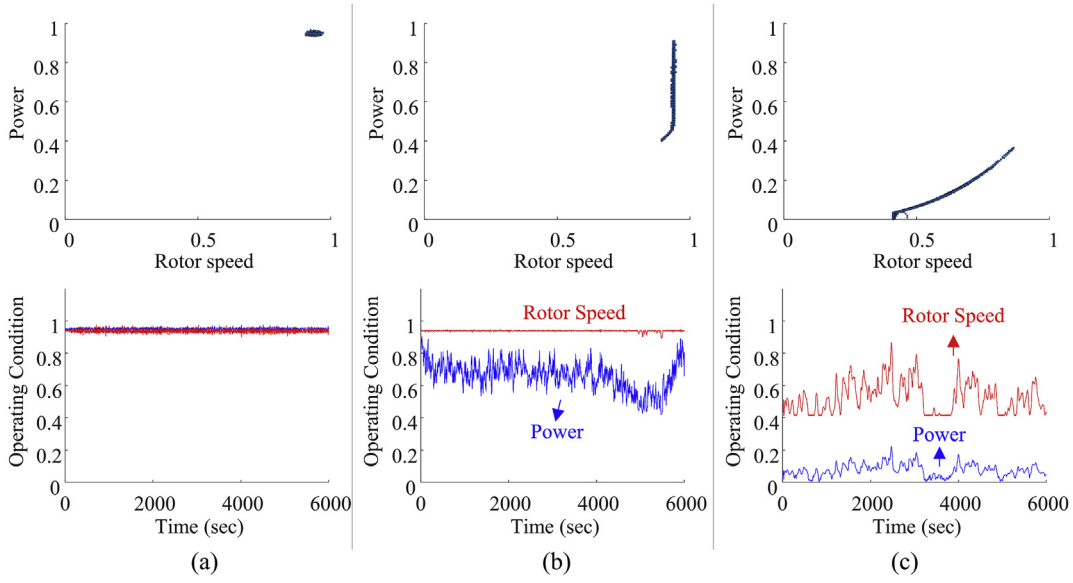

Fig. 14. Representative operating conditions for control of the WT testbed: (a) Class I, (b) Class II, (c) Class III.

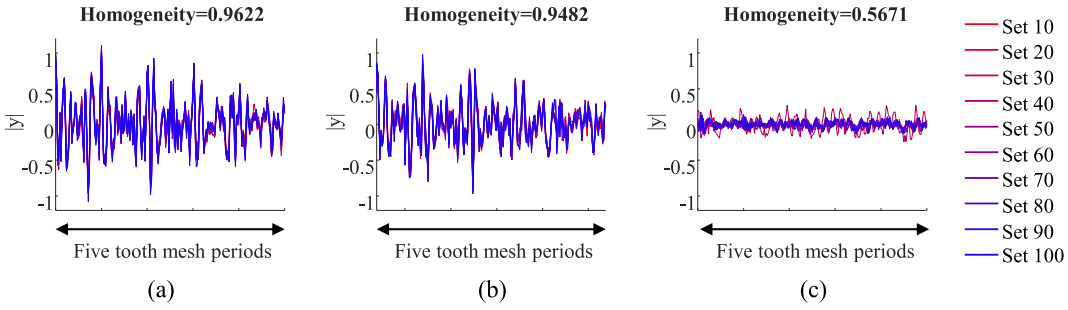

Fig. 15. Homogeneity evaluation results of the vibration signals: (a) Class I, (b) Class II, (c) Class III.

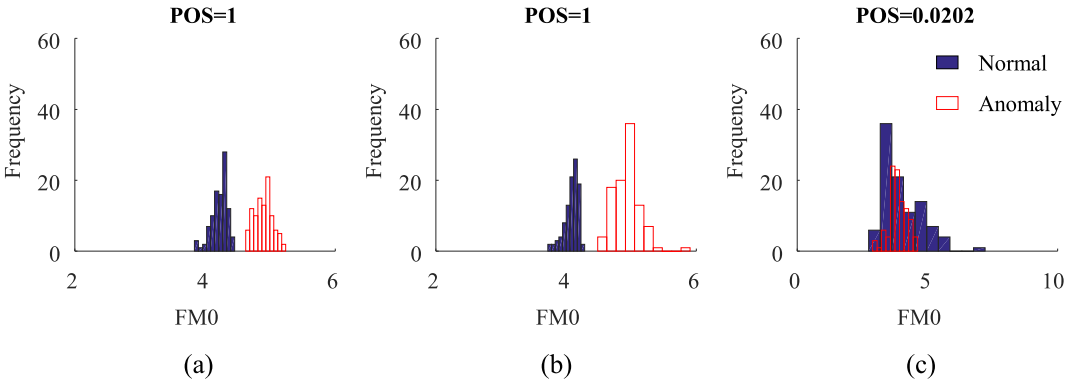

Fig. 16. *FM0* obtained from normal and anomaly conditions of the planetary gearbox: (a) Class I, (b) Class II, (c) Class III.

From these results, it can be concluded that variations in speed more significantly affect the level of homogeneity of vibration signals than do variations in power.

6.2. Vibration-based condition monitoring

To simulate an anomaly condition of the gearbox, a planet gear with spalling was manufactured as shown in the right side of Fig. 13. For fault diagnostics of the gearbox, fast Fourier transform analysis was employed along with autocorrelation-based time synchronous averaging (ATSA) [30]. Among various available condition indicators, *FM0* was used to evaluate the performance of the fault diagnostics results. *FM0*, which has been traditionally used for real-time condition monitoring of gearboxes, can be defined as [31]:

$$FM0_i = \frac{PP(ATSA_i)}{\sum_{k=1}^{N} A_i(f_k)} \tag{28}$$

where $ATSA_i$ represents the vibration signal in the ith dataset (v_i) processed with ATSA, $PP(ATSA_i)$ calculates the maximum peak-to-peak value of $ATSA_i$, and $A_i(f_k)$ denotes the amplitude of kth harmonic of the gear mesh frequency of $ATSA_i$.

Fig. 16 (a)~(c) compares the histograms of *FM0* values derived from the tests performed during both normal and anomaly conditions of the gearbox under the Class I, Class II, and Class III, respectively. To quantify the degree of separability, Fig. 16 indicates the probability of separation (POS), which gives one for perfect separation and zero for perfect overlap of PDFs from two classes [32]. In Class I and Class II, *FM0* from both the normal and anomaly conditions was clearly differentiated. This means that condition monitoring of the gearbox in Class I and Class II was feasible. In this case, the variation of the condition indicator in Class II was not large, despite the power variation. In Class III, *FM0* results from the normal and anomaly conditions were not perfectly separable, although there was some differentiation of overall magnitude between them.

7. Conclusions

Techniques for monitoring the condition of WTs have traditionally relied on the use of either stationary or non-stationary signals. However, to date, there has been no practical guideline outlining how to classify the operating condition of WTs for a class-wise condition monitoring purpose, and how to quantitatively define the ranges of the stationary operating condition of WTs. To address these challenges, this study devised a novel strategy to categorize the operating conditions of WTs using the empirical PDF and Gaussian mixture model (GMM).

An analytical WT model with a generic control logic is adopted to analyze the fundamental characteristics of operating conditions. This strategy was used because information about real-world control logic algorithms is proprietary and seldom released to the public. If available, a particular control logic for a real WT can be incorporated into the proposed method with only minor modifications. For example, for the case study using the WT in the field (See Fig. 11 (b)), the classification method and criteria could be revised to consider the considerable amount of the data around the cut-in rotor speed.

Based on the analysis of fundamental characteristics of operating conditions identified by the analytic WT model, a strategy is proposed to classify the operation condition of WTs into five classes. WTs are expected to have distinct operating properties at each class. Furthermore, quantitative classification criteria are defined using the empirical PDF-based method (Method 1) and a Gaussian mixture model (GMM)-based method (Method 2). Class I and II

data were extracted from WT signals using the proposed classification technique. For Class I and II data, the anomalous conditions of a gearbox in a WT testbed were clearly separated from the normal conditions through use of a low-cost signal processing technique (i.e., fast Fourier transform analysis with time synchronous averaging). With Class III data, there was overlap between the anomalous and normal conditions.

Method 2 requires considerable computational power for approximation of the optimal parameters for the GMM. The computational complexity of GMM is $O(KN_s^2)$ where K is the number of Gaussian distributions and N_s is the number of data points [36]. This challenge makes it difficult to update the classification criteria in real-time as more useful operating data are obtained. If the WT requires a real-time update of the classification criteria using big data while a high-power CPU is not available, thus, Method 1 would be more suitable for on-site utilization.

It is worth noting that the classification results of using Methods 1 and 2 can be inconsistent for different datasets. If both of Method 1 and 2 are available, it is recommended to adapt the method providing a lower level of criteria (C_p and C_w) to obtain the greatest data size used for the purpose of fault diagnostics, as long as the homogeneity of the signal is guaranteed.

From the case study, about 34% of data were classified into non-stationary operating condition classes, in which cost-efficient signal processing techniques cannot be effectively used for condition monitoring. It is worth noting that real data measured from a WT, about 120 min of data under the (quasi) stationary operating conditions (Class I and II) could be measured per day, on average. Thus, on average, 120 min of homogeneous condition monitoring signals are available for condition monitoring per day. Therefore, sufficient data exists such that, through the proposed method, an effective condition monitoring strategy can be implemented to support long-term operation and maintenance plans for WTs.

Acknowledgments

This work was supported by the Technology Innovation Program (10050980, System Level Reliability Assessment and Improvement for New Growth Power Industry Equipment) funded by the Ministry of Trade, Industry and Energy (MI, Korea).

References

[1] Z. Tian, T. Jin, B. Wu, F. Ding, Condition based maintenance optimization for wind power generation systems under continuous monitoring, Renew. Energy 36 (2011) 1502–1509.
[2] Z. Hameed, S.H. Ahn, Y.M. Cho, Practical aspects of a condition monitoring system for a wind turbine with emphasis on its design, system architecture, testing and installation, Renew. Energy 35 (2010) 879–894.
[3] P. Wang, P. Tamilselvan, J. Twomey, B.D. Youn, Prognosis-informed wind farm operation and maintenance for concurrent economic and environmental benefits, Int. J. Precis. Eng. Manuf. 14 (2013) 1049–1056.
[4] F.P. García Márquez, A.M. Tobias, J.M. Pinar Pérez, M. Papaelias, Condition monitoring of wind turbines: techniques and methods, Renew. Energy 46 (2012) 169–178.
[5] International Electrotechnical Commission (IEC), Wind Turbines: Communications for Monitoring and Control of Wind Power Plants - Logical Node Classes and Data Classes for Condition Monitoring, 2007.
[6] W. Yang, P.J. Tavner, C.J. Crabtree, Y. Feng, Y. Qiu, Wind turbine condition monitoring: technical and commercial challenges, Wind Energy 17 (2014) 673–693.
[7] L.F. Villa, A. Reñones, J.R. Perán, L.J. de Miguel, Statistical fault diagnosis based on vibration analysis for gear test-bench under non-stationary conditions of speed and load, Mech. Syst. Signal Process. 29 (2012) 436–446.
[8] Germanischer Lloyd (GL), Rules and Guidelines Industrial Services Part 4-guideline for the Certification of Condition Monitoring Systems for Wind Turbines, Germanischer Lloyd (GL), 2013.
[9] C.J. Crabtree, D. Zappala, P.J. Tavner, Survey of Commercially Available Condition Monitoring Systems for Wind Turbines, Technical Report of the University of Durham, 2011.
[10] Harry Timmerman, SKF WindCon - condition monitoring system for wind turbines, in: New Zealand Wind Energy Conference 2009, 2009.
[11] Acoem, Lifetime Reliability for Wind Turbines, Acoem group, 2012.
[12] K.E. Johnson, Adaptive Torque Control of Variable Speed Wind Turbines, National Renewable Energy Laboratory (NREL), 2008. TP-500–36265.
[13] T. Burton, D. Sharpe, N. Jenkins, E. Bossanyi, Wind Energy Handbook, second ed., John Wiley & Sons, 2001.
[14] E. Muljadi, C.P. Butterfield, Pitch-controlled variable-speed wind turbine generation, IEEE Trans. Ind. Appl. 37 (2001) 240–246.
[15] W. Hu, K.K. Choi, O. Zhupanska, J.H.J. Buchholz, Integrating variable wind load, aerodynamic, and structural analyses towards accurate fatigue life prediction in composite wind turbine blades, Struct. Multidiscip. Optim. 53 (3) (2015).
[16] Z. Xi, B.D. Youn, B.C. Jung, J.T. Yoon, Random field modeling with insufficient field data for probability analysis and design, Struct. Multidiscip. Optim. 51 (2015) 599–611.
[17] T. Jin, Z. Tian, Uncertainty analysis for wind energy production with dynamic power curves, in: 2010 IEEE 11th International Conference on Probabilistic Methods Applied to Power Systems, 2010, pp. 745–750.
[18] O. Rodriguez-Hernandez, O.A. Jaramillo, J.A. Andaverde, J.A. del Río, Analysis about sampling, uncertainties and selection of a reliable probabilistic model of wind speed data used on resource assessment, Renew. Energy 50 (2013) 244–252.
[19] J.F. Manwell, J.G. McGowan, A.L. Rogers, Wind Energy Explained: Theory, Design and Application, second ed., John Wiley & Sons, 2010.
[20] International Electrotechnical Commission (IEC), IEC 61400–1, Wind Turbine-part 1: Design Requirements, International Electrotechnical Commission (IEC), Switzerland, 2005.
[21] J.A. Gubner, Probability and Random Processes for Electrical and Computer Engineers, Cambridge University Press, 2006.
[22] L.F. Shampine, Vectorized adaptive quadrature in MATLAB, J. Comput. Appl. Math. 211 (2008) 131–140.
[23] M. Lydia, A.I. Selvakumar, S.S. Kumar, G.E.P. Kumar, Advanced algorithms for wind turbine power curve modeling, IEEE Trans. Sustain. Energy 4 (2013) 827–835.
[24] N. Baydar, A. Ball, Detection of gear deterioration under varying load conditions by using the instantaneous power spectrum, Mech. Syst. Signal Process. 14 (2000) 907–921.
[25] C.J. Stander, P.S. Heyns, W. Schoombie, Using vibration monitoring for local fault detection on gears operating under fluctuating load conditions, Mech. Syst. Signal Process. 16 (2002) 1005–1024.
[26] M.S. Waterman, D.E. Whiteman, Estimation of probability densities by empirical density functions†, Int. J. Math. Educ. Sci. Technol. 9 (1978) 127–137.
[27] A.W. van der Vaart, Asymptotic Statistics, Cambridge University Press, 2000.
[28] D. Reyanolds, Gaussian Mixture Models, Encyclopedia of Biometrics, 2009, pp. 659–663.
[29] R.A. Redner, H.F. Walker, Mixture densities, maximum likelihood and the EM algorithm, Soc. Ind. Appl. Math. 26 (1984) 195–239.
[30] J.M. Ha, B.D. Youn, H. Oh, B. Han, Y. Jung, J. Park, Autocorrelation-based time synchronous averaging for condition monitoring of planetary gearboxes in wind turbines, Mech. Syst. Signal Process. 70–71 (2016) 161–175.
[31] R.M. Stewart, Some Useful Data Analysis Techniques for Gearbox Diagnostics, MHM/R/10/77, Machine Health Monitoring Group, Institute of Sound and Vibration Research, University of Southampton, Southampton, 1977.
[32] B.C. Jeon, J.H. Jung, B.D. Youn, Y.-W. Kim, Y.-C. Bae, Datum unit optimization for robustness of a journal bearing diagnosis system, Int. J. Precis. Eng. Manuf. 16 (2015) 2411–2425.
[33] J.E. Bartlett, J.W. Kotrlik, C.C. Higgins, Organizational research: determining appropriate sample size in survey research, Information Technology, Learn. Perform. J. 19 (2001) 43–50.
[34] ASTM International, ASTM E122-07 Standard Practice for Calculating Sample Size to Estimate, with Specified Precision, the Average for a Characteristic of a Lot or Process, Annual Book of ASTM Standards, 2009, pp. 1–5.
[35] Y. Feng, Y. Qiu, C. Crabtree, H. Long, P. Tavner, Use of SCADA and CMS Signals for Failure Detection and Diagnosis of a Wind Turbine Gearbox, Ewea, 2011.
[36] Z. Chen, S. Haykin, J.J. Eggermont, S. Becker, Correlative Learning: a Basis for Brain and Adaptive Systems, Wiley, 2008.